

A LONG RANGE PHOTOGRAMMETRIC METHOD WITH ORTHOGONAL PROJECTION MODEL

Tetsu ONO*, Shin-ichi AKAMATSU*, Susumu HATTORI**

*Graduate School of Engineering, Kyoto University, Yoshida-Honmachi, Sakyo-ku, Kyoto 606-8501, JAPAN
ono@jf.gee.kyoto-u.ac.jp, akamatsu@info.gee.kyoto-u.ac.jp

**Faculty of Engineering, Fukuyama University, 1 Sanzo, Gakuen-cho, Fukuyama, 729-0292, JAPAN
hattori@fuip.fukuyama-u.ac.jp

KEY WORDS: photogrammetry, vision metrology, orthogonal projection, orientation model, long range observation

ABSTRACT

This paper describes a method appropriate for 3-D measurement from a long distance with a digital camera mounting a super telescopic lens. Long distance observation with telescopic lens camera is an effective method for displacement measurement such as small movement of top of a large cliff. However the conventional orientation method with the central perspective model widely used in close range photogrammetry is unstable in this case because of weak condition. In this study, an alternative model called the orthogonal projection model is applied. This model, which derived from the affine projection model with a constraint of orthogonality, is simple and better adapted to long distance observation. Furthermore, it is a great advantage that the orthogonal projection model does not require initial values of orientation parameters. In this study, the geometric characteristics of the orthogonal projection model were clarified by various simulations, and also the effectiveness of the method was verified by long distance field tests. Focal length of telescopic lens used in the field test was 400mm and distance to objects was over 100m. RMSE between the adjusted results with a camera and those with a totalstation was about 2.8mm. The accuracy with the proposed method is more than twice higher than that with the conventional method.

1 INTRODUCTION

In recent years digital close range photogrammetry has become applied to various objects in various fields. However it has not widely enough spread in fields of civil engineering and construction. In construction work, displacements of cliff faces or construction materials have to be precisely observed for disaster prevention, but ordinarily the target sites range over vast areas and moreover arrangement of view points is restricted. For example, movement of unstable rocks on top of large cliff has to be monitored to an accuracy of a few millimeters at ground points over 100m distant in some cases.

Close range photogrammetric techniques using camera with wide-angle lens are not available in these situations. Approaching the target objects is dangerous and may be impossible. It is not uncommon that fixing a deal of reflective targets on the objects is not allowed. In many cases, there is no alternative but to observe the object shape without clear marks from a distance. By using a telescopic lens camera, optical resolution can be kept high enough in spite of long distance observation. As focal length increased, however, view angle becomes smaller and geometric condition becomes worse. What is worse, available control points may be not many enough and may be ill-placed. Under these circumstances, the central perspective model generally used in close range photogrammetry is hardly applicable because of ill-posed problems.

Scaled orthographic projection models are widely used in computer vision to model the imaging process (Ullman 1979; Huang and Lee 1989; Tomasi and Kanade 1992; Shapiro et al 1995; Xu and Sugimoto 1999). They are mainly used for calculation of an approximation to perspective projection

model, but it should be noted that these models are stable in ill-conditions. Some papers in computer vision categorize them to the following camera models; the affine model, the weak perspective model and the para-perspective model.

The authors contrived the orthogonal projection model (Ono 2002), which belongs to the weak perspective model in the sense of camera model, but the basic concept is quite different from that of computer vision. The main aim of 3-D image analysis in computer vision is efficient estimation of motion. The weak perspective model is not a rigorous model but a approximate one in the real world. On the other hand, the orthogonal projection model is directly derived from the central perspective model without approximation. This model can provide an accurate solution by itself.

2 ORTHOGONAL PROJECTION MODEL

2.1 Basic concept

The conceptual diagram of orthogonal projection model is illustrated in Figure 1. The procedures of orthogonal projection model consist of the weak perspective projection and the projection transformation from the central perspective images.

From another viewpoint, this can be considered as a progressive model of the affine projection model, which Okamoto (1992,1998) proposed for long range observation.

2.2 Derivation of model equations

If the lens distortions and the shift of the principal points are negligible, the central perspective model is expressed

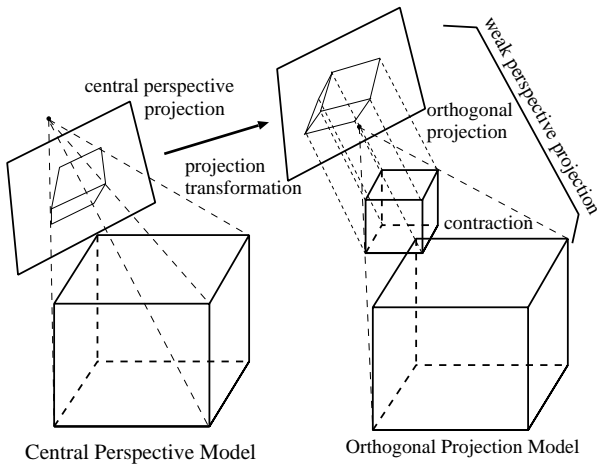


Figure 1: Conceptual diagram of orthogonal projection model

as:

$$\begin{pmatrix} x \\ y \\ -c \end{pmatrix} = \lambda \begin{pmatrix} a_{11} & a_{12} & a_{13} \\ a_{21} & a_{22} & a_{23} \\ a_{31} & a_{32} & a_{33} \end{pmatrix} \begin{pmatrix} X - X_o \\ Y - Y_o \\ Z - Z_o \end{pmatrix} \quad (1)$$

where λ is a scale factor, c is a principal distance, a_{ij} is components of rotation matrix and (X_o, Y_o, Z_o) is perspective center.

The value of λ changes in proportion to distance to object points. By substituting λ by constant scale parameter m , Equation (1) is described as :

$$\begin{pmatrix} x_a \\ y_a \\ -m/\lambda c \end{pmatrix} = m/\lambda \begin{pmatrix} x \\ y \\ -c \end{pmatrix} \quad (2)$$

$$= m \begin{pmatrix} a_{11} & a_{12} & a_{13} \\ a_{21} & a_{22} & a_{23} \\ a_{31} & a_{32} & a_{33} \end{pmatrix} \begin{pmatrix} X - X_o \\ Y - Y_o \\ Z - Z_o \end{pmatrix}$$

By transposing (X_o, Y_o, Z_o) to left site, equation (2) is described as following.

$$\begin{pmatrix} x_a - x_o \\ y_a - y_o \\ -m/\lambda c - z_o \end{pmatrix} = m \begin{pmatrix} a_{11} & a_{12} & a_{13} \\ a_{21} & a_{22} & a_{23} \\ a_{31} & a_{32} & a_{33} \end{pmatrix} \begin{pmatrix} X \\ Y \\ Z \end{pmatrix} \quad (3)$$

where

$$\begin{pmatrix} x_o \\ y_o \\ z_o \end{pmatrix} = m \begin{pmatrix} a_{11} & a_{12} & a_{13} \\ a_{21} & a_{22} & a_{23} \\ a_{31} & a_{32} & a_{33} \end{pmatrix} \begin{pmatrix} X_o \\ Y_o \\ Z_o \end{pmatrix}$$

The orthogonal projection with contraction is expressed by the first and second equations of (3).

$$\begin{aligned} x_a &= m\{a_{11}X + a_{12}Y + a_{13}Z\} + x_o \\ y_a &= m\{a_{21}X + a_{22}Y + a_{23}Z\} + y_o \end{aligned} \quad (4)$$

The number of independent parameters is six. They consist of x_o, y_o, m and three rotation angles.

Mathematically m is an arbitrary constant, which is involved with image coordinates x_a, y_a . From a practical standpoint, m is adjusted so as to scale down the average photographing distance to be same length as principal distance c (Figure 2).

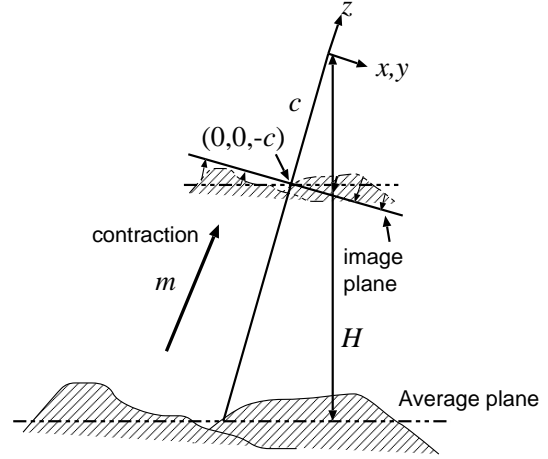


Figure 2: Constant scale parameter m

Let H be the average photographing distance to Z direction ($H = \bar{Z} - Z_o$), m is described as following.

$$m = -\frac{a_{33}c}{\bar{Z} - Z_o} = -\frac{a_{33}c}{H} \quad (5)$$

Equation (1) is reversely transformed as following.

$$\begin{pmatrix} X - X_o \\ Y - Y_o \\ Z - Z_o \end{pmatrix} = \frac{1}{\lambda} \begin{pmatrix} a_{11} & a_{21} & a_{31} \\ a_{12} & a_{22} & a_{32} \\ a_{13} & a_{23} & a_{33} \end{pmatrix} \begin{pmatrix} x \\ y \\ -c \end{pmatrix} \quad (6)$$

Taking notice of the third equation of (6), λ is expressed by:

$$\lambda = \frac{a_{13}x + a_{23}y - a_{33}c}{Z - Z_o} \quad (7)$$

By substituting (5) and (7) into (2), the equations of transformation from central perspective image coordinates to orthogonal projection ones are derived.

$$\begin{aligned} x_a &= \frac{Z - Z_o}{H} \frac{a_{33}c}{a_{33}c - a_{13}x - a_{23}y} x \\ y_a &= \frac{Z - Z_o}{H} \frac{a_{33}c}{a_{33}c - a_{13}x - a_{23}y} y \end{aligned} \quad (8)$$

Both of equations (4) and (8) are derived by the central perspective model without approximation. In this sense, the model consisting of (4) and (8) is as rigorous as the central perspective model.

2.3 Generalization of Orthogonal Projection Model

By simply generalizing equations (4), collinearity equations of affine projection model are derived.

$$\begin{aligned} x_a &= A_1X + A_2Y + A_3Z + A_4 \\ y_a &= A_5X + A_6Y + A_7Z + A_8 \end{aligned} \quad (9)$$

Addition of constraints for orthogonal projection to (9) leads to the generalized orthogonal projection model. Because

the generalized coefficients A_i ($i = 1, 2, 3, 5, 6, 7$) of equations (9) are derived from components of rotation matrix a_{ij} and scale parameter m , they have following features:

Constraint 1: vector (A_1, A_2, A_3) and (A_5, A_6, A_7) are perpendicular to each other.

Constraint 2: norm of (A_1, A_2, A_3) is equivalent to that of (A_5, A_6, A_7) .

Constraints 1 and 2 are described as:

$$A_1 A_5 + A_2 A_6 + A_3 A_7 = 0 \quad (10)$$

$$A_1^2 + A_2^2 + A_3^2 = A_5^2 + A_6^2 + A_7^2 \quad (11)$$

respectively. Constraint 1 means that an image plane and incident rays from objects are orthogonalized to each other. Constraint 2 means that scale of x_a direction is equivalent to that of y_a direction.

Affine projection model (9) with constraints (10) and (11) is defined as generalized orthogonal projection model. As mentioned above, orthogonal projection model has six independent orientation parameters. Two constraints reduce the degrees of freedom of equation (9) from 8 to 6 in generalized orthogonal projection model.

By generalizing the model, some advantages arise. Geometric orientation parameters of equation (4) are not linear to each other. This means that the initial values of unknowns are necessary just like the central perspective model. On the contrary, the orientation parameters of the generalized model are linear in equation (9). Equations of constraints are not linear, but there is no problem because equation (9) can give the approximation values. Furthermore, the generalized model has higher linear independence than the geometric model. Thus, the generalization of orthogonal projection model presumably conduces to robust adjustment.

From here, the generalized orthogonal projection model is treated as orthogonal projection model.

2.4 Estimation of Geometric Orientation Parameters

As mentioned above, orthogonal projection image coordinates (x_a, y_a) have to be transformed from observed image coordinates (x, y) . The transformation equation (8) requires values of components of rotation matrix a_{13}, a_{23}, a_{33} , Z, Z_o and c . These parameters can be estimated with the generalized parameters A_i .

Components of rotation matrix are estimated by following approaches. By definition of A_i ,

$$\begin{pmatrix} A_1 & A_2 & A_3 \\ A_5 & A_6 & A_7 \end{pmatrix} = m \begin{pmatrix} a_{11} & a_{12} & a_{13} \\ a_{21} & a_{22} & a_{23} \end{pmatrix} \quad (12)$$

Because norm of each line of rotation matrix is 1,

$$m^2 = A_1^2 + A_2^2 + A_3^2 \quad (13)$$

With equations (11) and (12), $a_{11}, a_{12}, a_{13}, a_{21}, a_{22}, a_{23}$, are easily determined. The other components a_{31}, a_{32}, a_{33} can be estimated by considering geometric feature of rotation matrix.

$$a_{11}^2 + a_{21}^2 + a_{31}^2 = 1$$

Thus

$$a_{31} = \pm \sqrt{1 - a_{11}^2 - a_{21}^2}$$

In the same way,

$$a_{32} = \pm \sqrt{1 - a_{12}^2 - a_{22}^2}$$

$$a_{33} = \pm \sqrt{1 - a_{13}^2 - a_{23}^2}$$

Furthermore,

$$\begin{aligned} a_{11}a_{31} + a_{12}a_{32} + a_{13}a_{33} &= 0 \\ a_{21}a_{31} + a_{22}a_{32} + a_{23}a_{33} &= 0 \end{aligned}$$

There are two sets of a_{31}, a_{32}, a_{33} which satisfy these all equations. A set closer to initial value is selected.

If c is given, Z_o is calculated with equation (6).

$$Z_o = \frac{a_{33}c}{m} + \bar{Z} \quad (14)$$

If precise value of c is unknown, compensation value Δc has to be calculated in collinearity equations. Even if X, Y, Z and A_i are correct, transformation errors by Δc cause large residuals of image coordinates. Conversely, Δc can be estimated from residuals of image coordinates. By equation (8) partial differential coefficients of x_a and y_a with respect to c are described as following.

$$\frac{\partial x_a}{\partial c} = \frac{Z - Z_o}{H} \frac{-a_{33}x(a_{13}x + a_{23}y)}{(a_{13}x + a_{23}y - a_{33}c)^2} \quad (15)$$

$$\frac{\partial y_a}{\partial c} = \frac{Z - Z_o}{H} \frac{-a_{33}y(a_{13}x + a_{23}y)}{(a_{13}x + a_{23}y - a_{33}c)^2} \quad (16)$$

By adding $\Delta x_a = \partial x_a / \partial c \Delta c$, $\Delta y_a = \partial y_a / \partial c \Delta c$ to equation (8), Δc can be adjusted as well as other unknowns.

2.5 Similarity to Object Space

Orthogonal projection image has a smaller number of indefinitenesses than affine projection one. Therefore it is conceivable that the 3-D model image constructed with overlapped orthogonal projection images has also a smaller number of indefinitenesses than 3-D affine model one.

For simplifying the problem, it is assumed that internal orientation parameters are known. The number of independent orientation parameters on stereo pair images is $6 \times 2 = 12$. By expressing with suffixes l and r to parameters of left and right images respectively, coplanarity condition of corresponding rays is described as following.

$$\begin{vmatrix} A_{1l} & A_{2l} & A_{3l} & A_{4l} - x_{al} \\ A_{5l} & A_{6l} & A_{7l} & A_{8l} - y_{al} \\ A_{1r} & A_{2r} & A_{3r} & A_{4r} - x_{ar} \\ A_{5r} & A_{6r} & A_{7r} & A_{8r} - y_{ar} \end{vmatrix} = 0 \quad (17)$$

By rearranging this equation, the following linear equation is derived.

$$x_{al} = B_1 y_{al} + B_2 x_{ar} + B_3 y_{ar} + B_4 \quad (18)$$

This shows that the coplanarity condition can mathematically provide 4 orientation parameters among the 12 ones of the stereo pair of orthogonal projection images. Hence, the number of the parameters determined by absolute orientation is $12 - 4 = 8$. This means that free network solutions by orthogonal projection model have $8 - 7 = 1$ indefiniteness against similarity to object space. In concrete terms, an angle between the corresponding rays of stereo pair images becomes indefinite, and the constructed space deforms to the depth direction.

In the next place, considering the orientation problem on the triplet orthogonal projection images, the number of orientation parameters is $6 \times 3 = 18$. On the other hand, the number of parameters determined by coplanarity condition is $4 \text{ times } 3 = 12$, but all of 12 parameters are not completely independent to each other. Because the following coplanarity condition with regard to all of three images is formed, one degree of freedom decreases.

$$x_{al} = C_1 y_{al} + C_2 y_{ar} + C_3 y_{ac} + C_4 \quad (19)$$

$C_i (i = 1, \dots, 4)$ are derived from 12 parameters of 3 coplanarity conditions. Therefore, the coplanarity conditions can mathematically provide $12 - 1 = 11$ orientation parameters. Thus, the degrees of freedom of the free network solutions are $18 - 11 = 7$. This means the free network 3D model space constructed with triplet orthogonal projection images has high similarity to objects.

Finally, the case where principal distance c is unknown is discussed. If c is unknown and fixed in triplet images, the number of unknown parameters increases to 19. As mentioned above, Δc can be estimated from residuals of image coordinates. In the other words, Δc can be determined by the coplanarity conditions. The number of parameters determined by coplanarity condition comes to be 12. Therefore, the degrees of freedom of the free network solutions come to be $19 - 12 = 7$. High similarity to the object space is retained in case where c is unknown and fixed.

3 SIMULATIONS

In order to investigate the geometrical characteristics of the orthogonal projection model, simple simulations were performed on the following cases.

1. stereo pair images are used and c is given
2. triplet images are used and c is given
3. triplet images are used and c is unknown

Configuration of camera and object points is illustrated in Figure 3 and Table 1.

Table 1: Coordinates of object points and camera position (mm)

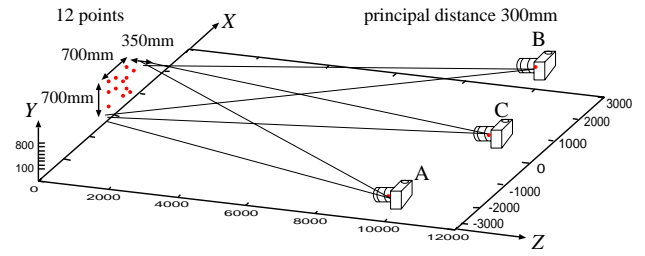


Figure 3: Configuration of camera and object points

No.	X	Y	Z
1	-200	800	0
2	-200	500	0
3	-300	100	0
4	-100	700	200
5	-150	350	300
6	100	700	0
7	50	450	0
8	250	800	350
9	300	550	0
10	250	250	250
11	400	800	0
12	400	150	0
A	-3000	500	10000
B	3000	400	10000
C	0	400	11000

Observed values and initial values were given by perturbing true values by normal random with the following standard deviations: 0.001mm in image coordinates, 10mm in object coordinates, 10mm in camera position, 2 degrees in inclination of camera.

3.1 Case 1

Only two images taken at point A and B were used. Principal distance c was fixed to true value 300mm.

The following indexes are shown in tables.

1. RMSE of image coordinates σ_0
 2. Internal errors
 3. RMSE between true values of object points and free network solutions transformed to center of objects by similar transformation
 4. RMSE between true values of object points and free network solutions transformed to center of objects by 3-D affine transformation
3. appreciates all deformations of obtained 3-D space, whereas 4. does not appreciate the overall deformation. By comparing values of 3. and 4., similarity to object space can be estimated.

Table 2: Results with stereo pair images (mm)

1	$\sigma_0 = 0.00169$			
	X	Y	Z	XYZ
2	0.0854	0.0836	0.1299	0.1019
3	0.9334	0.5566	2.2348	1.4347
4	0.0572	0.0849	0.0922	0.0796

3. has more than 10 times larger errors than 4. This result confirms that the orthogonal projection model cannot construct 3-D model with high similarity to the object space in case where only two overlapped images are used. Further, it is shown that indefiniteness appears in depth direction Z .

3.2 Case 2

Triplet images taken at point A, B and C were used. Principal distance c was fixed to the true value 300mm.

Table 3: Results with triplet images (mm)

1	$\sigma_0=$	0.00087			
	X	Y	Z	XYZ	
2	0.0417	0.0411	0.0647	0.0504	
3	0.0390	0.0499	0.0773	0.0577	
4	0.0258	0.0328	0.0599	0.0422	

Differences between 3. and 4. are small and the accuracies of both are high. It was confirmed that the proposed model is effective in the case where triplet images are used.

3.3 Case 3

Triplet images taken at point A, B and C were used. Principal distance c was fixed to the false value 290mm.

Table 4: The case where false value 290mm is given to c

1	$\sigma_0=$	0.00229			
	X	Y	Z	XYZ	
2	0.3014	0.2985	0.3892	0.3324	
3	0.1077	0.0884	0.2655	0.1731	
4	0.0350	0.0536	0.1170	0.0770	

The value of σ_0 was more than twice larger than that in the case 2. And the object coordinates were much worse than those in the case 2. This indicates that Δc affects residuals of image coordinates.

In the next test principal distance c was treated as unknown and the initial values 290mm was given to c .

Table 5: The case where c is treated as unknown

1	$\sigma_0=$	0.00083			
	X	Y	Z	XYZ	
2	0.0407	0.0401	0.0636	0.0494	
3	0.0682	0.0454	0.1072	0.0779	
4	0.0269	0.0216	0.0767	0.0485	

The obtained value of c was 299.3mm. Compared to the case where false value is given to c , the accuracy was obviously improved.

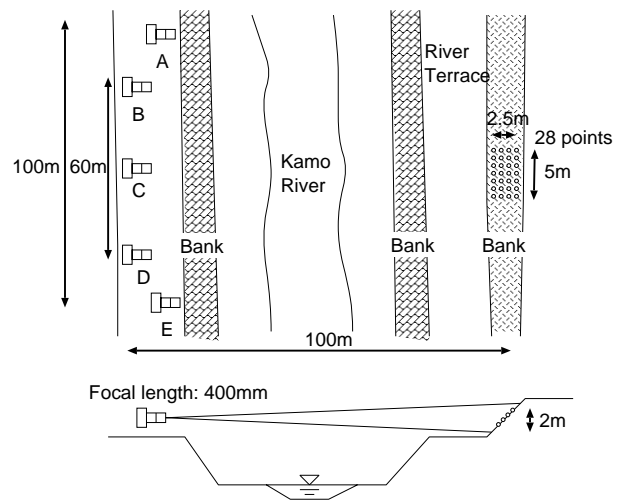


Figure 4: Configuration of camera and object points

4 FIELD TEST

A field test was carried out around Kamo-river at Kyoto Japan. Configuration of camera and object points is illustrated in Figure 4.

Conditions on the test are described below.

Camera: Canon D30 (Digital Camera equipped with CMOS sensor)

Image size: 2160 x 1440 pixels

Resolution: 10.5 μm / pixel

Lens: EF100-400mm F4.5-5.6L IS USM (Zoom lens)

Focal length: 400mm (fixed with tape)

Distance to objects: 100 – 110m

Target size: 2cm in diameter

The number of object points: 4 x 7 = 28

The number of images: 5



Figure 5: One of the photo images taken with D30

4.1 Bundle adjustment

The object coordinates was observed by the ground triangulation with a total-station as check data at the following accuracy.

Estimated standard errors: X:0.4767 Y:0.5031 Z:0.5173 (mm)

Initial values of object coordinates were calculated by re-sampling the check data by 50cm. Initial values of orientation parameters were estimated with the initial values of object coordinates by using DLT.

For comparison purpose, free network bundle adjustments were performed with both of the central perspective model and the orthogonal projection model.

c was treated as unknown. Zeros were given to the other internal orientation parameters.

4.2 Results

Two tests with different number of images were carried out. The indexes mentioned at previous section were calculated with both of the two models in each test.

Table 6: Results with 5 images (mm)

central perspective model				
1	$\sigma_0=$	0.002611		
	X	Y	Z	XYZ
3	7.9642	2.6021	6.2955	6.0507
4	2.1044	0.7834	3.4743	2.3884
orthogonal projection model				
1	$\sigma_0=$	0.002658		
	X	Y	Z	XYZ
3	3.4556	1.0566	3.4874	2.8994
4	2.1074	0.7836	3.4505	2.3777

Table 7: Results with 3 images (B,C,D) (mm)

central perspective model				
1	$\sigma_0=$	0.002633		
	X	Y	Z	XYZ
3	99.5854	43.8100	96.2873	83.8805
4	3.8363	1.3900	6.7535	4.5555
orthogonal projection model				
1	$\sigma_0=$	0.002755		
	X	Y	Z	XYZ
3	9.8375	3.9887	9.4912	8.2213
4	2.1514	0.9260	4.8342	3.1014

These results show that the orthogonal projection model is more effective than the central perspective model for long distance observation. Especially, the proposed model is robust in bad condition.

5 CONCLUSIONS

This paper described the principles of the orthogonal projection model, which is appropriate for long distance observation. In addition, the following several characteristics on the proposed model were confirmed by some simulations and a field test.

- The proposed model can achieve higher accuracy than the conventional model on long distance observation.

- More than three overlapped images are required for accurate adjustment with the proposed model.
- Principal distance c can be self-calibrated with the proposed model.
- Initial values of orientation parameters are not necessary for adjustment with the proposed model. They can be estimated with a small number of control points.

REFERENCES

Abdel-Aziz, Y.A. and Karara, H.M. (1971), Direct linear transformation from comparator coordinates into object space coordinates, Sympo. Close-Range Photogrammetry, American Society of Photogrammetry, pp.1-18

Huang, T.S. and Lee, C.H. (1989), Motion and Structure From Orthographic Projections, IEEE Trans. Pattern Analysis and Machine Intelligence, Vol.11, pp.536-540

Okamoto, A. et al (1998), General Orientation Problem Of Totalstation Zoom-lens CCD Camera Imagery, Proceedings of ASPRS-RTI 1998 Annual Conference, pp.44-57

Okamoto, A. (1992), Ultra-precise measurement using affine transformation, International Archives of Photogrammetry and Remote Sensing, Vol.29, Commission V, pp.318-322

Ono, T. Hattori, S (2002), Fundamental Principles of Image Orientation Using Orthogonal Projection Model, International Archives of Photogrammetry and Remote Sensing, Vol.31, B3/1, pp.611-615

Osuni, J. and Dunn, S. (1996), Motion From Three Weak Perspective Images Using Image Rotation, IEEE Trans. Pattern Analysis and machine Intelligence, Vol.18, No.1, pp.64-69.

Shapiro, L.S., Zisserman, A. et al (1995), 3D Motion Recovery via Affine Epipolar Geometry, International Journal of Computer Vision, 16, pp.147-182.

Tomasi, C. and Kanade, T. (1992), Shape and Motion From Image Streams under orthography: a factorization method, International Journal of Computer Vision, 9(2), pp.137-154.

Ulman, S. (1979), The Interpretation of Visual Motion, Cambridge, MA: MIT Press.

Xu, G. and Sugimoto, N. (1999), A Linear Algorithm for Motion From Three Weak Perspective Images Using Euler Angles, IEEE Trans. Pattern Analysis and Machine Intelligence, Vol.21, No.1, pp.54-57